

ZegOT: Zero-shot Segmentation Through Optimal Transport of Text Prompts

Kwanyoung Kim^{*1} Yujin Oh^{*1} Jong Chul Ye¹

Abstract

Recent success of large-scale Contrastive Language-Image Pre-training (CLIP) has led to great promise in zero-shot semantic segmentation by transferring image-text aligned knowledge to pixel-level classification. However, existing methods usually require an additional image encoder or retraining/tuning the CLIP module. Here, we present a cost-effective strategy using text-prompt learning that keeps the entire CLIP module frozen while fully leveraging its rich information. Specifically, we propose a novel **Zero-shot segmentation with Optimal Transport (ZegOT)** method that matches multiple text prompts with frozen image embeddings through optimal transport, which allows each text prompt to efficiently focus on specific semantic attributes. Additionally, we propose Deep Local Feature Alignment (DLFA) that deeply aligns the text prompts with intermediate local feature of the frozen image encoder layers, which significantly boosts the zero-shot segmentation performance. Through extensive experiments on benchmark datasets, we show that our method achieves the state-of-the-art (SOTA) performance with only $\times 7$ lighter parameters compared to previous SOTA approaches.

1. Introduction

Zero-shot Semantic Segmentation (ZS3) is one of label-efficient approach for dense prediction task, which reduce efforts for expensive pixel-level annotations of unseen object categories (Bucher et al., 2019). Vision language models (VLM) such as CLIP (Radford et al., 2021) have brought great advance in ZS3 task by transferring pre-trained image-text aligned knowledge to pixel-text level category matching problems (Ding et al., 2022; Xu et al., 2021; Zhou et al., 2022a; Rao et al., 2022; Zhou et al., 2022d). The key idea

^{*}Equal contribution ¹School of AI, Korea Advanced Institute of Science and Technology (KAIST), Daejeon, Republic of Korea. Correspondence to: Jong Chul Ye <jong.ye@kaist.ac.kr>.

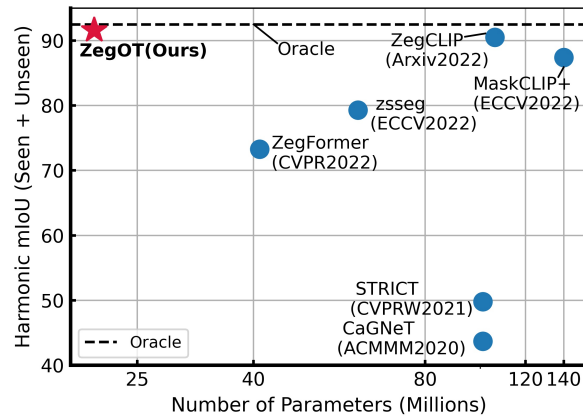


Figure 1. Harmonic mean IoU of various zero-shot semantic segmentation methods over the number of learnable parameters on PASCAL VOC dataset. Black dashed line indicates the fully supervised learning result of ours.

here is to use the VLM knowledge gained through contrastive learning on large-scale image-text pairs through a special knowledge transfer process tailored to ZS3.

Suppose that our goal is to learn a functional map that transfers the pre-trained image-level domain \mathcal{X} knowledge to the novel pixel-level domain \mathcal{Y} . To achieve this goal, various approaches have been explored by training additional models or leveraging a novel domain knowledge, as indicated in Table 1. In general, existing ZS3 approaches based on pre-trained VLM can be categorized into two groups: Frozen image encoder with learnable proposal generator-based approaches (FE) (Ding et al., 2022; Xu et al., 2021), and trainable image encoder-based approaches (TE) covering re-training or fine-tuning (Rao et al., 2022; Zhou et al., 2022d).

FE approaches exploit the \mathcal{Y} domain knowledge through image information from the proposal generator. These approaches utilize the capability of image-level classification in the frozen image encoder. A major drawback of FE approaches is that they require an additional trainable image encoder to generate region proposals, which leads to high-cost memory complexity. Also, FE performance is highly dependent on the frozen VLM, which is not tailored for pixel-level dense prediction. On the other hand, TE ap-

Table 1. Systemic analysis of ZegOT compared to baseline CLIP-based semantic segmentation models.

Model	Proposal generator	CLIP module retrain/fine-tune	Additional backbone	Multiple text prompt	#Params
ZegFormer (Ding et al., 2022)	✓	✗	✗	✗	41M
zsseg (Xu et al., 2021)	✓	✗	✗	✗	61M
DenseCLIP (Rao et al., 2022)	✗	✓	✗	✗	105M
ZegCLIP (Zhou et al., 2022d)	✗	✓	✗	✗	130M
MaskCLIP+ (Zhou et al., 2022a)	✗	✗	✓	✗	140M
ZegOT (ours)	✗	✗	✗	✓	21M

proaches explicitly address the VLM dependency issue by directly training another image encoder for dense prediction and exploiting \mathcal{Y} domain knowledge through class-driven text information. Compared to FE approaches, leveraging novel domain knowledge through textual information is simple and efficient in terms of complexity. Since TE approaches are learned for a specific domain, they achieve superior performance compared to FE approaches for the corresponding ZS3 task. However, TE approaches also suffer from high computational cost due to the learnable image encoder.

One naive solution could be to let the image decoder and text prompt as only learnable parts, while keeping the VLM image encoder and text encoder frozen. However, this solution is problematic because the text prompt and image embedding are not effectively aligned since it only utilizes global alignment between image-text.

To address this, here we present a cost-effective framework with learnable multiple text prompts which fully exploits both the global and local alignment between vision and language features from deep layers of the frozen VLM without further re-training or tuning (see Table 1). However, in the frozen VLM setting, simply introducing the multiple text prompts is problematic, since the learned text prompts can be converged to represent similar semantic features. Surprisingly, we found that optimal transport (OT) theory can provide a solution, by allowing each prompt to efficiently focus on different semantic features, producing optimally aligned pixel-text score maps. The aligned score map by OT can tolerate domain shift between different class distributions, leading to robust segmentation performance on unseen classes. More specifically, we initially optimize the optimal transport plan between multiple text prompts and the frozen image embeddings on seen classes, and then utilize the optimized transport plan to predict pixel-text score maps for both seen and unseen classes. This allows us to achieve the state-of-the-art (SOTA) performance on both seen and unseen classes, as shown in Fig. 1.

Our contributions can be summarized as:

- We propose a cost-effective ZegOT that learns multiple text-prompts while keeping the entire VLM frozen, which allows our model to fully leverage highly aligned

vision and language information for zero-shot semantic segmentation tasks.

- In ZegOT, the proposed multi prompt optimal transport solver module closely matches the distribution between image embeddings from the frozen VLM and the learnable text-prompts despite its cost-effectiveness.
- Through extensive experiments on three benchmark datasets, we demonstrate that our ZegOT achieves SOTA performance for zero-shot semantic segmentation tasks while requiring only $\times 7$ fewer parameters compared to the previous SOTA approach.

2. Related Work

2.1. Zero-shot Semantic Segmentation

Semantic segmentation for large-scale vocabulary needs a labor-intensive pixel-level annotation process, which leads a label-imbalance issue, *i.e.*, not all the categories from the large vocabulary are annotated in the training dataset. Zero-shot semantic segmentation (ZS3) solves this label-imbalance problem by generalizing labeled (seen) class knowledge to predict new (unseen) class information (Bucher et al., 2019). Recent success of CLIP (Radford et al., 2021) accelerates advancement of ZS3 performance by utilizing aligned knowledge between the image encoder and the class-driven text encoder. Zhou et al. (Zhou et al., 2022d) successfully bridges the performance gap between the seen and unseen classes by utilizing CLIP model as a backbone feature extractor for dense-level image-text alignment.

ZS3 can be performed by either inductive or transductive settings. Compared to traditional inductive zero-shot setting where class names and pixel-level annotations of unseen classes are both unavailable during training (Ding et al., 2022), a newly introduced transductive setting boosts the ZS3 performance by utilizing unseen class names and self-generated pseudo labels guided by the model itself during training (Gu et al., 2020; Xu et al., 2021; Pastore et al., 2021; Zhou et al., 2022d;a). Accordingly, our ZegOT basically follows the transductive ZS3 setting.

2.2. Prompt Learning

Prompt learning was initially introduced in the field of Natural Language Processing (NLP), which efficiently adapts large-scale model knowledge to various downstream tasks. Rather than using traditional self-supervised learning paradigm, *i.e.*, pre-train and fine-tune the large-scale model to transfer the knowledge to downstream tasks, the prompt learning formulates the downstream adjustment problem by training light-weight optimal textual prompts (Petroni et al., 2019; Shin et al., 2020; Jiang et al., 2020; Liu et al., 2021).

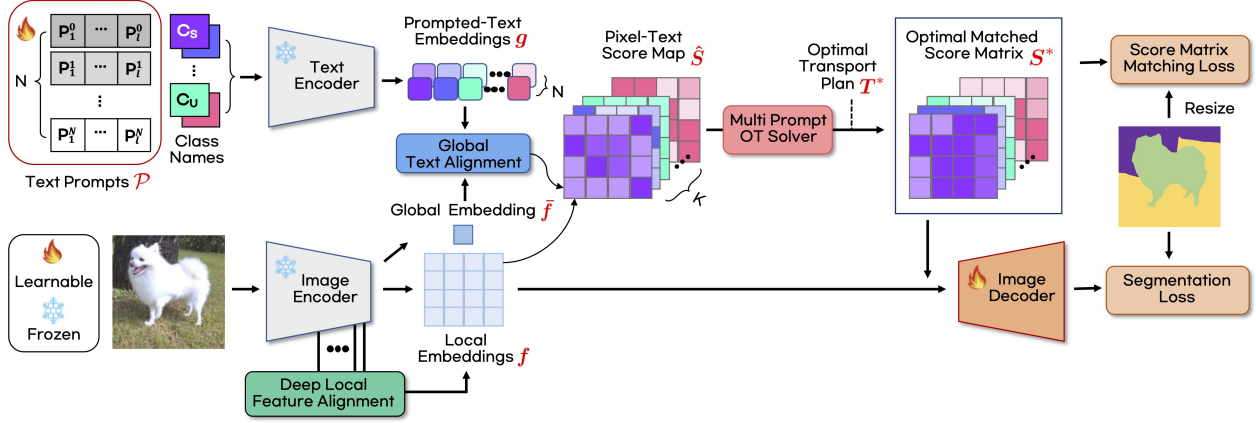


Figure 2. Overall pipeline of our proposed ZegOT for zero-shot semantic segmentation. The only learnable parts are the multiple text prompts \mathcal{P} and the image decoder, while entire CLIP encoder modules are frozen.

Compared to the fine-tuning method, text prompts-driven downstream adaptation is efficient, but still alleviates the domain shift problem that occurs between the pre-trained domain and the downstream domain. Recently, introducing a set of learnable text prompts into the frozen VLM achieved superior performance in various computer vision (CV) tasks (Zhou et al., 2022c;b; Gao et al., 2021; Rao et al., 2022). Visual Prompt Tuning (VPT) is also a novel solution that introduces trainable image prompts to each layer of a transformer encoder (Jia et al., 2022), which can be transferred to various downstream tasks (Zang et al., 2022; Sohn et al., 2022; Liu et al., 2022). However, VPT requires high memory consumption, which is comparable to the re-training method. Our method uses only text prompts to adapt to the ZS3 task, which leads to a memory-efficient advantage.

2.3. Optimal Transport

Optimal transport (OT) is a general mathematical framework to evaluate correspondences between two distributions. Thanks to the luminous property of distribution matching, the optimal transport has received great attention in various computer vision tasks, such as domain adaptation (Flamary et al., 2016), semantic correspondence problem (Liu et al., 2020), graph matching (Xu et al., 2019a;b), and cross-domain alignment (Chen et al., 2020), etc. Among various methods, Sinkhorn algorithm can efficiently solve the OT problem through entropy-regularization (Cuturi, 2013), and it can be directly applied to deep learning frameworks thanks to the extension of Envelop Theorem (Peyré et al., 2019). Prompt Learning with Optimal Transport (PLOT) (Chen et al., 2022) is mostly related to ours, which optimizes the optimal transport distance to align visual features and text features by the Sinkhorn algorithm given trainable multiple text prompts. However, PLOT only considers a few-shot

image classification problem, while we apply the optimal transport theory to a zero-shot dense prediction problem to focus on specific attributes of semantic objects, which facilitates ZS3.

3. Methods

As illustrated in Fig. 2, our proposed ZegOT is composed of frozen text/image encoder modules with trainable text prompts, a global text alignment (GTA) module, an image decoder module and a multi prompt optimal transport solver (MPOT) module. A primary goal of ZegOT is to segment objects belongs to both seen classes \mathcal{C}_S and unseen classes \mathcal{C}_U , i.e., $\mathcal{C} = \mathcal{C}_S \cup \mathcal{C}_U$, under the transductive ZS3 setting. Note that $\mathcal{C}_S \cap \mathcal{C}_U = \emptyset$ and both annotations and class names of \mathcal{C}_S are available, but the only class names of \mathcal{C}_U are known during training. We introduce two novel methods into ZegOT to learn dense vision-language alignment in a cost-effective way: 1) prompt-guided deep text-pixel alignment and 2) multi prompt optimal transport solver.

3.1. Prompt-guided Deep Text-Pixel Alignment

Multiple Text Prompt Learning To fully leverage the CLIP pre-trained knowledge, we make N text prompts $\mathcal{P} = \{\mathbf{P}^i\}_{i=1}^N$ as only trainable context tokens from the text encoder module. i.e., $\mathbf{P}^i = [P_1^i, P_2^i, \dots, P_l^i]$, where l denotes the length of the context tokens. The randomly initialized multiple text prompts \mathcal{P} are identically prepended to K tokenized class names as $\mathcal{T} = \{\{\mathcal{P}, \mathbf{c}^k\}\}_{k=1}^K$, where $\{\mathbf{c}^k\}_{k=1}^K \subset \mathcal{C}$ is the word embedding of each class name. Note that the text prompts \mathcal{P} are shared throughout all the class names.

Now, an input image is encoded through the frozen CLIP image encoder layer to yield the i -th intermediate local

image embedding $\mathbf{f}_i \in \mathbb{R}^{H_L W_L \times D}$, $i = 1, \dots, L$ from the i -th hidden image encoder layer, where H_L and W_L are the height and width of the local image embeddings from L -th layer and D denotes the embedding dimension. We further define global image embedding $\bar{\mathbf{f}}_L \in \mathbb{R}^{1 \times D}$. Using these, we define variants of desirable pixel-text aligned score matrices as:

$$\hat{\mathbf{S}}_i = \mathbf{f}_i \mathbf{g}_{GA}^\top, \quad \mathbf{S}_i^* = \mathbf{T}_i^* \odot \hat{\mathbf{S}}_i, \quad (1)$$

where the superscript \top refers to the transpose operation, $\mathbf{S}_i^* \in \mathbb{R}^{H_L W_L \times KN}$ is the refined score matrix by optimal transport map \mathbf{T}_i^* which will be discussed in Sec 3.2. Furthermore,

$$\mathbf{g}_{GA} = \mathcal{Q}(\text{cat}[\bar{\mathbf{f}}_L \odot \mathbf{g}, \mathbf{g}]) \in \mathbb{R}^{KN \times D}$$

is the globally aligned text embedding where \mathcal{Q} denotes a linear layer for matching the concatenated embedding dimension to the original dimension D , cat is the concatenation operator, and \odot is the Hadamard product, and $\mathbf{g} = E_{\text{text}}(\mathcal{T}) \in \mathbb{R}^{KN \times D}$ denotes the text embeddings from the N -prompted class names \mathcal{T} , where E_{text} is the frozen text encoder. Finally, \mathbf{f}_i , $\bar{\mathbf{f}}_L$, \mathbf{g} and \mathbf{g}_{GA} are \mathcal{L}_2 normalized along the embedding dimension.

The score matrices in (1) can be either directly matched to the pixel-level annotation labels, or fed into the image decoder as an intermediate feature to predict segmentation maps as:

$$\hat{\mathbf{Y}} = D_\theta(\text{cat}[\{\mathcal{M}(\hat{\mathbf{S}}_i)_{i=1}^L\}, \mathcal{M}(\hat{\mathbf{S}}_L)]), \quad (2)$$

$$\mathbf{Y}^* = D_\theta(\text{cat}[\{\mathcal{M}(\hat{\mathbf{S}}_i)_{i=1}^L\}, \mathcal{M}(\mathbf{S}_L^*)]). \quad (3)$$

where $\hat{\mathbf{Y}}, \mathbf{Y}^* \in \mathbb{R}^{HW \times K}$ and $\mathcal{M}: \mathbb{R}^{H_L W_L \times KN} \rightarrow \mathbb{R}^{H_L W_L \times K}$ is the operation which first reshape $\mathbb{R}^{H_L W_L \times KN} \rightarrow \mathbb{R}^{H_L W_L \times K \times N}$ and perform summation the matrix along the N dimension. *e.g.*, $\mathcal{M}(\hat{\mathbf{S}}_i) \in \mathbb{R}^{H_L W_L \times K}$, D_θ is the trainable image decoder, and H and W are the height and width of image, respectively. Accordingly, $\hat{\mathbf{Y}}$ is the prediction of our baseline model, and \mathbf{Y}^* is the prediction of ZegOT. The used notation is summarized in Table 5 of Appendix B.

In Eqs. (2) and (3), the operations $\hat{\mathbf{S}}_i$ and $\{\mathcal{M}(\hat{\mathbf{S}}_i)_{i=1}^L\}$ are so important that they are specially referred to Global Text Alignment (GTA) and Deep Local Feature Alignment (DLFA), respectively. In the following, we describe them in more detail.

Global Text Alignment (GTA) The local image embeddings \mathbf{f}_L inherently contain the text-image aligned knowledge of CLIP. However, when pre-training, the global image embedding $\bar{\mathbf{f}}_L$ and the text embeddings \mathbf{g} comprise the cosine similarity score which is maximized through contrastive learning so that $\bar{\mathbf{f}}_L$ contains richer pixel-text aligned information than \mathbf{f}_L . Thus, we further exploit $\bar{\mathbf{f}}_L$ in the GTA

module to compute the score matrix $\hat{\mathbf{S}}_L \in \mathbb{R}^{H_L W_L \times KN}$ by employing an idea of relation descriptor method (Zhou et al., 2022d) in (1).

Deep Local Feature Alignment (DLFA) Meanwhile, Feature Pyramid Network (FPN) (Lin et al., 2017) is a common choice for segmentation decoder, where high-level semantic features from deep encoder layers comprise a latent feature for the following image decoder. Our ZegOT also adopts FPN, but we fully align the extracted intermediate local embeddings from the frozen image encoder with the globally aligned text embedding \mathbf{g}_{GA} . In other words, we extend the idea of GTA to all the intermediate local embeddings, *i.e.*, $\{\hat{\mathbf{S}}_i\}_{i=1}^L$, where $\hat{\mathbf{S}}_i \in \mathbb{R}^{H_L W_L \times KN}$ is the i -th score matrix. Through the simple arithmetic calculation, the entire hidden image embeddings extracted from the frozen CLIP encoder can be deeply aligned with both the global image and text embeddings without any further learnable parameters.

3.2. Multi Prompt Optimal Transport Solver

Optimal Transport Problem Optimal transport aims to minimize the transport distance between two probability distributions. In this paper, we only consider discrete distribution which is closely related to our framework. We assume that discrete empirical distributions μ and ν are defined on probability space $\mathcal{F}, \mathcal{G} \in \Omega$, respectively, as follows:

$$\mu = \sum_{i=1}^M p_i \delta_{f_i}, \quad \nu = \sum_{j=1}^N q_j \delta_{g_j}, \quad (4)$$

where δ_f and δ_g denote Dirac functions centered on \mathbf{f} and \mathbf{g} , respectively, M and N denote the dimension of the empirical distribution. The weight vectors $\mathbf{p} = \{p_i\}_{i=1}^M$ and $\mathbf{q} = \{q_j\}_{j=1}^N$ belong to the M and N -dimensional simplex, respectively, *i.e.*, $\sum_{i=1}^M p_i = 1$, $\sum_{j=1}^N q_j = 1$. The discrete optimal transport problem can be then formulated as:

$$\begin{aligned} \mathbf{T}^* &= \arg \min_{\mathbf{T} \in \mathbb{R}^{M \times N}} \sum_{i=1}^M \sum_{j=1}^N T_{ij} C_{ij} \\ \text{s.t. } \mathbf{T} \mathbf{1}^N &= \mu, \quad \mathbf{T}^\top \mathbf{1}^M = \nu. \end{aligned} \quad (5)$$

Here, \mathbf{T}^* is called the optimal transport plan, which is learned to minimize the total distance between the two probability vectors. \mathbf{C} is the cost matrix which represents the distance between \mathbf{f}_i and \mathbf{g}_j , *e.g.*, the cosine distance $C_{ij} = 1 - \frac{\mathbf{f}_i \mathbf{g}_j^\top}{\|\mathbf{f}_i\|_2 \|\mathbf{g}_j\|_2}$, and $\mathbf{1}^M$ refers to the M -dimensional vector with ones.

However, solving the problem (5) costs $O(n^3 \log n)$ -complexity (n proportional to M and N), which is time-consuming. This issue can be efficiently solved by entropy-regularizing the objective, called the Sinkhorn-Knopp (or

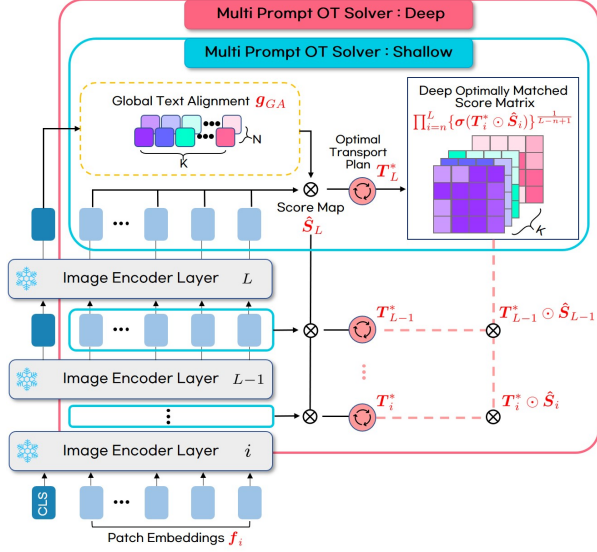


Figure 3. A schematic diagram of Multi Prompt Optimal Transport (MPOT) solvers including Shallow and Deep variants.

simply Sinkhorn) algorithm (Cuturi, 2013). In Sinkhorn algorithm, the optimization problem is reformulated as:

$$\begin{aligned} \mathbf{T}^* = \arg \min_{\mathbf{T} \in \mathbb{R}^{M \times N}} \sum_{i=1}^M \sum_{j=1}^N \mathbf{T}_{ij} \mathbf{C}_{ij} - \lambda H(\mathbf{T}) \\ \text{s.t. } \mathbf{T} \mathbf{1}^N = \boldsymbol{\mu}, \quad \mathbf{T}^\top \mathbf{1}^M = \boldsymbol{\nu}. \end{aligned} \quad (6)$$

where $H(\mathbf{T}) = \sum_{ij} \mathbf{T}_{ij} \log \mathbf{T}_{ij}$ and $\lambda > 0$ is the regularization parameter. The problem (6) is a strictly convex optimization problem, and thus we have an optimization solution with fewer iterations as follows:

$$\mathbf{T}^* = \text{diag}(\mathbf{a}^t) \exp(-\mathbf{C}/\lambda) \text{diag}(\mathbf{b}^t) \quad (7)$$

where t is the iteration and $\mathbf{a}^t = \boldsymbol{\mu} / \exp(-\mathbf{C}/\lambda) \mathbf{b}^{t-1}$ and $\mathbf{b}^t = \boldsymbol{\nu} / \exp(-\mathbf{C}/\lambda) \mathbf{a}^t$, with the initialization on $\mathbf{b}^0 = \mathbf{1}$.

Multiple Prompt OT Solver (MPOT) To incorporate the OT theory into our framework, we define the total cost matrix \mathbf{C} in (6) using the globally aligned score matrix $\hat{\mathbf{S}}_i$ in (1), *i.e.*, for the i -th layer, we set $\mathbf{C} := \mathbf{C}_i = \mathbf{1} - \hat{\mathbf{S}}_i$, where $\mathbf{C}_i \in \mathbb{R}^{H_L W_L \times KN}$ denotes the i -th cost matrix. Given the cost matrix \mathbf{C}_i , the goal of MPOT is to obtain the corresponding optimal transport plan $\mathbf{T}_i^* \in \{\mathbf{T}_i^*\}_{i=1}^L$ as Eq. (7) (Here, $M = H_L W_L$, $N = KN$ in (6) and the algorithm in Appendix D), which is a mapping matrix that maximizes the cosine similarity between the frozen image embedding and the learnable multiple prompts-derived text embeddings. Depending on the depth of incorporating image encoder layers for the optimization process, we have two ZegOT variants, *i.e.*, ZegOT-Shallow and ZegOT-Deep, as shown in Fig. 3.

ZegOT-Shallow As illustrated in Fig 3, ZegOT-Shallow calculate optimal transport plan $\mathbf{T}_L^* \in \mathbb{R}^{H_L W_L \times KN}$ in L -th layer. Since our goal is to obtain a pixel-text score matrix that minimizes the total distance between the two image and text embedding spaces, we can reformulate the final score matrix as :

$$\mathbf{S}_L^* = \mathbf{T}_L^* \odot \hat{\mathbf{S}}_L \quad (8)$$

where \mathbf{S}_L^* is the refined score matrix with transport plan \mathbf{T}_L^* in L -th layer. Then, we can obtain the prediction of ZegOT-Shallow \mathbf{Y}^* by plugging (8) into (3).

ZegOT-Deep Instead of optimizing the transport plan \mathbf{T}_L^* just for the single layer as in Eq. (8), ZegOT-Deep leverages intermediate image embeddings from the deep image encoder layers to yield multiple transport plans $\{\mathbf{T}_i^*\}_{i=n}^L$, where $\mathbf{T}_i \in \mathbb{R}^{H_L W_L \times KN}$ and n denotes the starting layer that comprises the multiple transport plans. We apply geometric mean among the multiple transport plans to reflect the knowledge of intermediate score matrices as follows:

$$\mathbf{S}_L^* = \prod_{i=n}^L \sigma\{\mathbf{S}_i^*\}^{\frac{1}{d}}, \quad \mathbf{S}_i^* = \mathbf{T}_i^* \odot \hat{\mathbf{S}}_i \quad (9)$$

where $d = L - n + 1$ denotes the depth of incorporating image encoder layers, σ is the sigmoid function if $n \leq i < L$, and the identity function otherwise (since intensity range of all the score matrix is $(-1, 1)$, we conduct Sigmoid for all the intermediate image embeddings except for the last layer). Accordingly, in ZegOT-Deep, the model prediction \mathbf{Y}^* can be obtained by plugging (9) into (3).

Note that Eq. (7) only contains matrix multiplication and exponential operation, *i.e.*, the calculations are fully differentiable, thus the gradients can be back-propagated throughout the entire neural network.

3.3. Training Procedure and Inference

As discussed in Section 3, ZegOT follows the transductive ZS3 setting. Similar to the previous SOTA methods (Zhou et al., 2022d;a), the entire training schedule is divided into three phases: Seen classes-guided learning, Pseudo label-guided learning, and Self-training. For each phase, ground-truth labels for unseen classes are updated, *i.e.*, ZegOT self-generates labels at once or continuously (see the details of the training phases are described in Appendix C).

Loss Function In this work, we combine three different losses which is similar to previous methods as follows:

$$\mathcal{L}_{\text{total}} = \lambda_{\text{CE}} \mathcal{L}_{\text{CE}} + \lambda_{\text{fc}} \mathcal{L}_{\text{fc}} + \lambda_{\text{dc}} \mathcal{L}_{\text{dc}}, \quad (10)$$

$$\mathcal{L}_{\text{seg}} = \mathcal{L}_{\text{total}}(\mathbf{Y}^*, \mathbf{Y}^{\text{gt}}), \quad (11)$$

$$\mathcal{L}_{\text{score}} = \mathcal{L}_{\text{total}}(\mathcal{M}(\mathbf{S}_L^*), \mathcal{R}_d(\mathbf{Y}^{\text{gt}})) \quad (12)$$

where $\mathcal{L}_{\text{total}}$ denotes the total loss combining different three losses, *i.e.*, \mathcal{L}_{CE} is the cross entropy loss, \mathcal{L}_{fc} is the focal loss, and \mathcal{L}_{dc} is the dice loss, with λ_{CE} , λ_{fc} , and λ_{dc} as corresponding hyper-parameters. \mathcal{L}_{seg} is the segmentation loss and $\mathcal{L}_{\text{score}}$ is the score matrix matching loss, where $\mathbf{Y}^* \in \mathbb{R}^{HW \times K}$, $\mathcal{M}(\mathbf{S}_L^*) \in \mathbb{R}^{H_L W_L \times K}$ are the predictions of our model, $\mathcal{R}_d : \mathbb{R}^{HW \times K} \rightarrow \mathbb{R}^{H_L W_L \times K}$ is the down-sampling operator ($H_L W_L < HW$), and $\mathbf{Y}^{\text{gt}} \in \mathbb{R}^{HW \times K}$ is the ground-truth label.

In the training phase, the following two optimization problems are updated as :

$$\min_{\{\mathbf{P}^i\}_{i=1}^N} \mathcal{L}_{\text{prompt}} = \lambda_{\text{seg}} \mathcal{L}_{\text{seg}} + \lambda_{\text{score}} \mathcal{L}_{\text{score}}, \quad (13)$$

$$\min_{D_\theta} \mathcal{L}_{\text{Decoder}} = \lambda_{\text{seg}} \mathcal{L}_{\text{seg}} \quad (14)$$

where $\mathcal{L}_{\text{prompt}}$ and $\mathcal{L}_{\text{Decoder}}$ denote the losses for each the learnable mutiple text prompts and the image decoder, λ_{seg} and λ_{score} are hyper-parameters. The details of the loss function are described in Appendix E.

Inference Since we optimize both \mathbf{Y}^* and \mathbf{S}_L^* , we compute the final segmentation output $\mathbf{Y}^*_{\text{final}}$ by jointly leveraging the decoder output \mathbf{Y}^* and the score matrix \mathbf{S}_L^* as:

$$\mathbf{Y}^*_{\text{final}} = (1 - w) \cdot \mathbf{Y}^* + w \cdot \mathcal{R}_{\text{up}}(\mathbf{S}_L^*). \quad (15)$$

where $w \in [0, 1]$ denotes the hyper-paramter for controlling the balance between \mathbf{Y}^* and \mathbf{S}_L^* , and $\mathcal{R}_{\text{up}} : \mathbb{R}^{H_L W_L \times K} \rightarrow \mathbb{R}^{HW \times K}$ is the upampling operator.

4. Experiments

4.1. Dataset and Evaluation Metric

Dataset To evaluate the effectiveness of our proposed method, we carry out extensive experiments on three challenging datasets: PASCAL VOC 2012 (Everingham & Winn, 2012), PASCAL Context (Mottaghi et al., 2014), and COCO-Stuff164K (Caesar et al., 2018). To fairly compare with previous methods (Bucher et al., 2019; Xu et al., 2021; Ding et al., 2022; Zhou et al., 2022a;d), we follow the identical protocol of dividing seen and unseen classes for each dataset. The dataset details are described in Appendix F.

Evaluation Metric By following previous works, we measure the mean of class-wise intersection over union (mIoU) on both seen and unseen classes, indicated as mIoU(S) and mIoU(U), respectively. We adopt the harmonic mean IoU (hIoU) of seen classes and unseen classes as a major metric. More details of the definition are deferred to Appendix H. We also report the pixel-wise classification accuracy (pAcc) in Appendix I.

4.2. Implementation Details

We implement the proposed method on the open-source toolbox MMSegmentation¹ and conducted it on 4 RTX-3090 GPUs with batch size of 16. We adopt the pre-trained CLIP ViT-B/16 model² as the frozen encoder module and adopt FPN which is equipped with atrous spatial pyramid pooling (ASPP) (Chen et al., 2017) module as the image decoder for all the experiments. Further details are deferred to Appendix G. We will release our source code for reproduction.

4.3. Experimental Results

Zero-shot Semantic Segmentation Fig. 4 shows the qualitative zero-shot segmentation performance of our ZegOT and the baseline method. Among the transductive methods, our ZegOT-Deep segments semantic objects most accurately on both PASCAL VOC and PASCAL Context datasets. Specifically, both our ZegOT-Shallow and ZegOT-Deep show superior performance on sectioning semantic boundaries of unseen objects compared to MaskCLIP+. Quantitative results are also presented in Table 2. Our ZegOT-Deep achieves the SOTA performance for most datasets. For the largest COCO-Stuff-164K dataset, our ZegOT produces comparable qualitative segmentation results compared to the previous SOTA methods, as shown in Fig. 7 of Appendix K. The drop in quantitative performance in Table 2 for this dataset is because, compared to the retraining/fine-tuning methods, our current lightweight decoder with limited trainable parameters may be insufficient to be directly applied to the large-scale dataset. We expect this issue may be solved in a future study, by increasing the size of trainable model parameters.

OT-driven Text Prompt-Image Alignment To explore the origin of the superior segmentation performance of our ZegOT-Deep, we further analyze our proposed multi-prompt OT solver by visualizing each text prompt-related score matrix in Fig. 5. For comparison, we set a multi-prompt baseline which basically shares ZegOT structure but the OT solver module is ablated. In the baseline method, all the text prompts \mathcal{P} -related score matrices in Fig. 5 strikingly resemble each others, which implies that the multiple text prompts are converged to learn similar semantics. On the other hand, in ZegOT-Shallow, the multiple text prompts focus on different attributes of the target object, achieving fine-grained text-pixel alignment. However, a certain text prompt (\mathbf{P}^4 for each) tends to focus on background pixels rather than the foreground object. In ZegOT-Deep, each text prompt not only attends to different attributes, but a certain text prompt (\mathbf{P}^2 for each) effectively highlights boundaries of the target object, which suggests that the model takes

¹<https://github.com/open-mmlab/mms Segmentation>

²<https://github.com/openai/CLIP>

Table 2. Quantitative comparison of zero-shot semantic segmentation performance of ZegOT with baseline methods on PASCAL VOC 2012, PASCAL Context, and COCO-Stuff 164K datasets.

Settings	Methods	PASCAL VOC 2012			PASCAL Context			COCO-Stuff164K			#Params
		mIoU (S)	mIoU (U)	hIoU	mIoU (S)	mIoU (U)	hIoU	mIoU (S)	mIoU (U)	hIoU	
Inductive (Seen supervised)	CaGNet (Gu et al., 2020)	78.4	26.6	39.7	24.1	18.5	21.2	35.5	12.2	18.2	101M
	ZegFormer (Ding et al., 2022)	86.4	63.6	73.3	-	-	-	36.6	33.2	34.8	41M
	zsseg (Xu et al., 2021)	83.5	72.5	77.5	-	-	-	39.3	36.3	36.3	61M
	ZegCLIP (Zhou et al., 2022d)	91.9	77.8	84.3	46.0	54.6	49.9	40.2	41.4	40.8	130M
Transductive w/ Self Training (Seen supervised + Unseen self-supervised)	CaGNet (Gu et al., 2020)	78.6	30.3	43.7	-	-	-	35.6	13.4	19.5	101M
	STRICT (Pastore et al., 2021)	82.7	35.6	49.8	-	-	-	35.3	30.3	32.6	101M
	zsseg (Xu et al., 2021)	79.2	78.1	79.3	-	-	-	38.1	43.6	41.5	61M
	MaskCLIP+ (Zhou et al., 2022a)	88.1	86.1	87.4	48.1	66.7	53.3	39.6	54.7	45.0	140M
	ZegCLIP (Zhou et al., 2022d)	92.3	89.9	91.1	46.8	68.5	55.6	40.6	59.9	48.4	130M
	ZegOT-Shallow (Ours)	91.8	87.3	89.5	51.1	72.5	59.9	37.9	49.2	42.8	21M
	ZegOT-Deep (Ours)	91.9	91.6	91.7	50.5	72.5	59.5	37.6	49.0	42.5	21M
Fully-supervised (Oracle)	ZegCLIP (Zhou et al., 2022d)	92.4	90.9	91.6	46.5	78.7	56.9	40.7	63.2	49.6	130M
	ZegOT-Shallow (Ours)	92.1	91.9	92.0	51.6	73.5	60.6	38.3	58.7	46.4	21M
	ZegOT-Deep (Ours)	92.0	91.6	91.8	50.9	73.6	60.2	38.1	58.3	46.1	21M

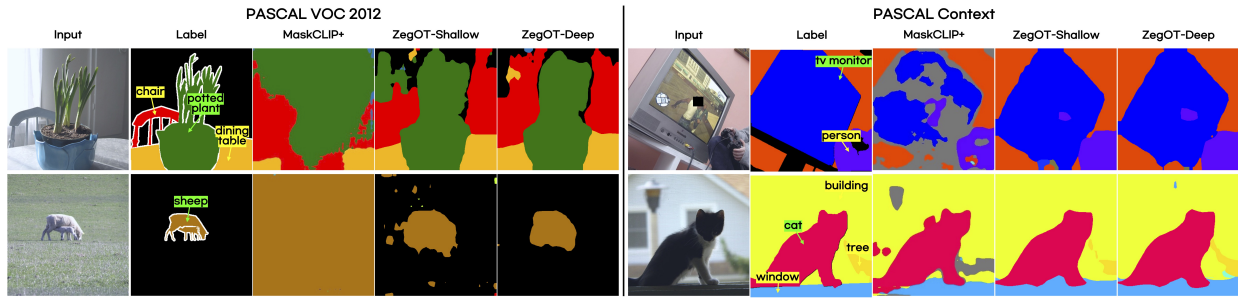
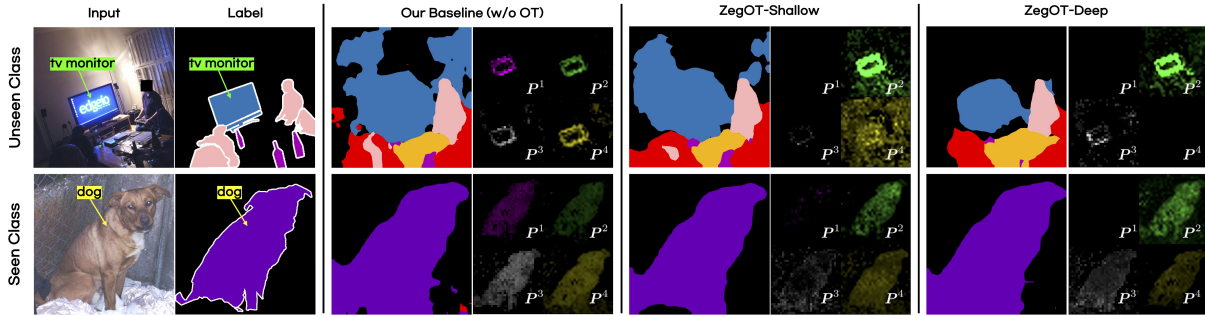


Figure 4. Qualitative zero-shot segmentation results on PASCAL VOC 2012 and PASCAL Context datasets. The yellow tag indicates seen classes, while the green tag indicates unseen classes.


 Figure 5. Visualization of the learned text prompt and image pixel alignment. For each method, we present its segmentation result (left) and N multiple text prompts-related score matrix activated by the predicted class (right). In the baseline method without OT, all the P^i -related score matrices resemble each others. On the other hand, our ZegOT-Shallow and ZegOT-Deep show separate score matrices, with ZegOT-Deep more focusing on different semantic attributes of the predicted class object.

advantage of all the learned text prompts for improving segmentation performance. Additional visualization of the text prompts-driven score matrices are provided in Fig. 9 of Appendix K.

Analysis on Deep Text Feature Alignment To demonstrate the effectiveness of the proposed DLFA, we conduct in-depth analysis comparing the strength of feature align-

ment with or without DLFA on PASCAL VOC 2012 dataset. Fig. 6 shows the bar plot of average text-pixel alignment given a specific class name over the image encoder layer index. To calculate the strength of feature alignment, we extract the score matrices $\{\hat{S}_i\}_{i=1}^L$ for a certain class name (e.g., dog) and calculate the average \hat{S}_i along entire pixels for each image encoder layer. We find that the strength of feature alignment with DLFA is much higher compared

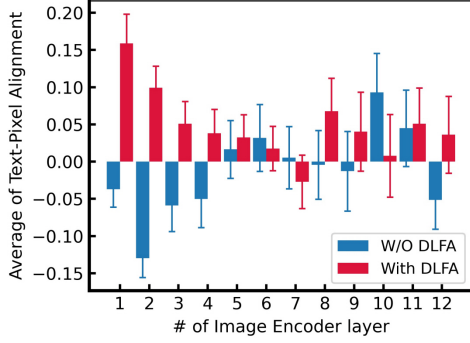


Figure 6. Bar plots of the average pixel-text alignment versus the image encoder layer index given a specific class name with or without Deep Local Feature Alignment (DLFA).

to that without DLFA in almost layers. In particular, the average value of text-pixel alignment significantly increases at the earlier layers and the final layer. The result confirms that our model with DLFA effectively exploits the activated alignment between the two language-text modalities.

4.4. Ablation Studies

Network Module Analysis To demonstrate the effectiveness of our proposed DLFA and MPOT modules, we further conduct ablation studies on PASCAL VOC 2012 dataset as reported in Table 3. Firstly, our baseline method without the DLFA module shows a drastic drop in performance on the unseen class, with a margin of -16.9% and -10.2% for each mIoU(U) and hIoU. The result suggests that our DLFA module efficiently transfers pre-trained CLIP knowledge to the deep local features to yield better text-pixel alignment under the ZS3 setting. Next, we study the effect of the MPOT solver variants. In general, we observe that our MPOT brings improvement on unseen classes, while performances on seen classes are comparable throughout the entire method. Our ZegOT-Shallow outperforms the baseline by a margin of +1.9% mIoU(U) and +1.0% hIoU. Moreover, our ZegOT-Deep boosts by mIoU(U) +6.2% and hIoU +3.2% compared to the baseline, and these results are even comparable to the results of Oracle which is trained in a fully supervised manner. We confirm that the proposed structure with optimal transport framework certainly takes advantage of improving performance under the ZS3 setting.

Effect of Hyper-parameters of Network Components

To further investigate the effect of network components, we conduct the component analysis on hyper-parameter as shown in Table 4. Firstly, we observe the segmentation performance by varying the total number N of the learnable text prompts. We empirically find that ZegOT performs

Table 3. Analysis of network module contribution.

Model	DLFA	MPOT	mIoU(S)	mIoU(U)	hIoU
Our Baseline	✗	✗	91.3	68.5(-16.9)	78.3(-10.2)
	✓	✗	91.9	85.4	88.5
ZegOT-Shallow	✓	Shallow	91.8	87.3(+1.9)	89.5(+1.0)
ZegOT-Deep	✓	Deep	91.9	91.6(+6.2)	91.7(+3.2)
Oracle	✓	Deep	92.0	91.6	91.8

Table 4. Component analysis of hyper-parameters. # denotes the hyper-parameters of configurations. Checkmark ✓ indicates the default configuration of ZegOT-Shallow and ZegOT-Deep.

Components	#	mIoU (S)	mIoU (U)	hIoU	ZegOT
Number of text prompts	2	91.6	82.9	87.0	
	4	91.9	91.6	91.7	✓
	6	91.8	89.6	90.7	
Depth of MPOT	12	91.8	87.3	89.5	✓ -Shallow
	10-12	91.4	87.3	89.3	
	8-12	91.9	91.6	91.7	✓ -Deep
	4-12	91.6	90.2	90.9	
	1-12	92.1	86.5	89.3	

the best when $N = 4$, but the performance drops when N is decreased to 2 or increased to 6, which implies that fewer text prompts are insufficient to learn comprehensive semantic features, whereas too many text prompts complicate the optimal transport matching process. We further explore the effect of the depth of MPOT solver, *i.e.*, ranges of the frozen image encoder layers that inserted to MPOT. Although inserting multiple layers to MPOT boosts performance, it also causes performance trade-off between seen and unseen classes segmentation. We find that introducing the MPOT with 8 to 12-th layers of the image encoder achieves the best performance, which becomes the default setting of ZegOT-Deep for the entire experiments.

5. Conclusion

In this work, we proposed ZegOT, a cost-effective segmentation framework that optimizes multiple text prompts by utilizing a frozen visual-language model, which thoroughly leverages the aligned vision-language knowledge for zero-shot semantic segmentation tasks. We also incorporated optimal transport theory into our framework to train multiple text prompts for representing different semantic properties. We demonstrated that our ZegOT outperforms the SOTA zero-shot segmentation approaches on various benchmark datasets with the lightest model parameters. Our in-depth analyses also confirmed that our ZegOT effectively delivered performance gains on both seen and unseen classes.

References

- Bucher, M., Vu, T.-H., Cord, M., and Pérez, P. Zero-shot semantic segmentation. *Advances in Neural Information Processing Systems*, 32, 2019.
- Caesar, H., Uijlings, J., and Ferrari, V. Coco-stuff: Thing and stuff classes in context. In *Proceedings of the IEEE conference on computer vision and pattern recognition*, pp. 1209–1218, 2018.
- Chen, G., Yao, W., Song, X., Li, X., Rao, Y., and Zhang, K. Prompt learning with optimal transport for vision-language models. *arXiv preprint arXiv:2210.01253*, 2022.
- Chen, L., Gan, Z., Cheng, Y., Li, L., Carin, L., and Liu, J. Graph optimal transport for cross-domain alignment. In *International Conference on Machine Learning*, pp. 1542–1553. PMLR, 2020.
- Chen, L.-C., Papandreou, G., Kokkinos, I., Murphy, K., and Yuille, A. L. Deeplab: Semantic image segmentation with deep convolutional nets, atrous convolution, and fully connected crfs. *IEEE transactions on pattern analysis and machine intelligence*, 40(4):834–848, 2017.
- Cuturi, M. Sinkhorn distances: Lightspeed computation of optimal transport. *Advances in neural information processing systems*, 26, 2013.
- Ding, J., Xue, N., Xia, G.-S., and Dai, D. Decoupling zero-shot semantic segmentation. In *Proceedings of the IEEE/CVF Conference on Computer Vision and Pattern Recognition*, pp. 11583–11592, 2022.
- Everingham, M. and Winn, J. The pascal visual object classes challenge 2012 (voc2012) development kit. *Pattern Anal. Stat. Model. Comput. Learn., Tech. Rep.*, 2007: 1–45, 2012.
- Flamary, R., Courty, N., Tuia, D., and Rakotomamonjy, A. Optimal transport for domain adaptation. *IEEE Trans. Pattern Anal. Mach. Intell.*, 1, 2016.
- Gao, P., Geng, S., Zhang, R., Ma, T., Fang, R., Zhang, Y., Li, H., and Qiao, Y. Clip-adapter: Better vision-language models with feature adapters. *arXiv preprint arXiv:2110.04544*, 2021.
- Gu, Z., Zhou, S., Niu, L., Zhao, Z., and Zhang, L. Context-aware feature generation for zero-shot semantic segmentation. In *Proceedings of the 28th ACM International Conference on Multimedia*, pp. 1921–1929, 2020.
- Jia, M., Tang, L., Chen, B.-C., Cardie, C., Belongie, S., Hariharan, B., and Lim, S.-N. Visual prompt tuning. *arXiv preprint arXiv:2203.12119*, 2022.
- Jiang, Z., Xu, F. F., Araki, J., and Neubig, G. How can we know what language models know? *Transactions of the Association for Computational Linguistics*, 8:423–438, 2020.
- Lin, T.-Y., Dollár, P., Girshick, R., He, K., Hariharan, B., and Belongie, S. Feature pyramid networks for object detection. In *Proceedings of the IEEE conference on computer vision and pattern recognition*, pp. 2117–2125, 2017.
- Liu, L., Yu, B. X., Chang, J., Tian, Q., and Chen, C.-W. Prompt-matched semantic segmentation. *arXiv preprint arXiv:2208.10159*, 2022.
- Liu, X., Zheng, Y., Du, Z., Ding, M., Qian, Y., Yang, Z., and Tang, J. Gpt understands, too. *arXiv preprint arXiv:2103.10385*, 2021.
- Liu, Y., Zhu, L., Yamada, M., and Yang, Y. Semantic correspondence as an optimal transport problem. In *Proceedings of the IEEE/CVF Conference on Computer Vision and Pattern Recognition*, pp. 4463–4472, 2020.
- Mottaghi, R., Chen, X., Liu, X., Cho, N.-G., Lee, S.-W., Fidler, S., Urtasun, R., and Yuille, A. The role of context for object detection and semantic segmentation in the wild. In *Proceedings of the IEEE conference on computer vision and pattern recognition*, pp. 891–898, 2014.
- Pastore, G., Cermelli, F., Xian, Y., Mancini, M., Akata, Z., and Caputo, B. A closer look at self-training for zero-label semantic segmentation. In *Proceedings of the IEEE/CVF Conference on Computer Vision and Pattern Recognition*, pp. 2693–2702, 2021.
- Petroni, F., Rocktäschel, T., Lewis, P., Bakhtin, A., Wu, Y., Miller, A. H., and Riedel, S. Language models as knowledge bases? *arXiv preprint arXiv:1909.01066*, 2019.
- Peyré, G., Cuturi, M., et al. Computational optimal transport: With applications to data science. *Foundations and Trends® in Machine Learning*, 11(5-6):355–607, 2019.
- Radford, A., Kim, J. W., Hallacy, C., Ramesh, A., Goh, G., Agarwal, S., Sastry, G., Askell, A., Mishkin, P., Clark, J., et al. Learning transferable visual models from natural language supervision. In *International Conference on Machine Learning*, pp. 8748–8763. PMLR, 2021.
- Rao, Y., Zhao, W., Chen, G., Tang, Y., Zhu, Z., Huang, G., Zhou, J., and Lu, J. Denseclip: Language-guided dense prediction with context-aware prompting. In *Proceedings of the IEEE/CVF Conference on Computer Vision and Pattern Recognition*, pp. 18082–18091, 2022.

- Shin, T., Razeghi, Y., Logan IV, R. L., Wallace, E., and Singh, S. Autoprompt: Eliciting knowledge from language models with automatically generated prompts. *arXiv preprint arXiv:2010.15980*, 2020.
- Sohn, K., Hao, Y., Lezama, J., Polania, L., Chang, H., Zhang, H., Essa, I., and Jiang, L. Visual prompt tuning for generative transfer learning. *arXiv preprint arXiv:2210.00990*, 2022.
- Xu, H., Luo, D., and Carin, L. Scalable gromov-wasserstein learning for graph partitioning and matching. *Advances in neural information processing systems*, 32, 2019a.
- Xu, H., Luo, D., Zha, H., and Duke, L. C. Gromov-wasserstein learning for graph matching and node embedding. In *International conference on machine learning*, pp. 6932–6941. PMLR, 2019b.
- Xu, M., Zhang, Z., Wei, F., Lin, Y., Cao, Y., Hu, H., and Bai, X. A simple baseline for zero-shot semantic segmentation with pre-trained vision-language model. *arXiv preprint arXiv:2112.14757*, 2021.
- Zang, Y., Li, W., Zhou, K., Huang, C., and Loy, C. C. Unified vision and language prompt learning. *arXiv preprint arXiv:2210.07225*, 2022.
- Zhou, C., Loy, C. C., and Dai, B. Extract free dense labels from clip. In *European Conference on Computer Vision*, pp. 696–712. Springer, 2022a.
- Zhou, K., Yang, J., Loy, C. C., and Liu, Z. Conditional prompt learning for vision-language models. In *Proceedings of the IEEE/CVF Conference on Computer Vision and Pattern Recognition*, pp. 16816–16825, 2022b.
- Zhou, K., Yang, J., Loy, C. C., and Liu, Z. Learning to prompt for vision-language models. *International Journal of Computer Vision*, 130(9):2337–2348, 2022c.
- Zhou, Z., Zhang, B., Lei, Y., Liu, L., and Liu, Y. Zegclip: Towards adapting clip for zero-shot semantic segmentation. *arXiv preprint arXiv:2212.03588*, 2022d.

A. Limitations and Negative Societal Impacts

Limitations Our model performance is highly dependent on the CLIP model knowledge. Specially, the class name-driven unseen object segmentation can be failed, unless the CLIP model is pre-trained with the target class-related image-text pairs.

Negative Societal Impacts Our paper has a potential privacy issue in providing visual results of the person class. To avoid the issue, every person in all the figures are properly anonymized by covering the faces.

B. Notation

We provide a summary of notation in Table 5

C. Zero-shot Segmentation Training Process.

By following the general transductive zero-shot semantic segmentation (ZS3) setting (Pastore et al., 2021; Zhou et al., 2022a;d), we divide the entire training procedure into 3 phases, and the label \mathbf{Y}^{gt} is phase-adaptively altered for training the unseen classes, as described in Algorithm 1.

Phase 1. Seen Class Supervised Training For the first 1/10 training iterations, the model is trained utilizing the ground truth label \mathbf{Y}^{gt} , which only contains pixel-wise labels $\mathbf{Y}_{hw}^{\text{gt}}$ for seen classes \mathcal{C}_S , and the rest labels are ignored for calculating losses.

Phase 2. Unseen Class Pseudo-label Guided Training Once the network is trained, the learned knowledge can be transferred to update the labels for unseen classes \mathcal{C}_U . Since the learnable decoder is optimized for the seen class-only, we only utilize score matrix \mathbf{S}^* for updating each pixel value of the ground truth label $\mathbf{Y}_{hw}^{\text{gt}}$ which not belongs to \mathcal{C}_S , while keeping original labels for \mathcal{C}_S . Then, the model is trained utilizing the updated pseudo-label, until reaching the half of the training iterations.

Phase 3. Unseen Class Self Training For the rest of the training iterations, the model self-generates each pixel values of the ground truth label $\mathbf{Y}_{hw}^{\text{gt}}$ which not belongs to \mathcal{C}_S , at every training iteration.

D. Optimal Transport algorithm

E. Details of Loss function

As discussed in Section 3.3, we combine three different losses, including Cross Entropy (CE) loss, the focal loss based on Binary Cross Entropy (BCE) loss, and the dice

Algorithm 1 ZegOT Pseudo-code

Input: ZegOT model Z_t at iteration t , The subset of seen classes \mathcal{C}_S and unseen classes \mathcal{C}_U , e.g, $\mathcal{C}_S \cap \mathcal{C}_U = \emptyset$. The training dataset $D = \{(x, \mathbf{Y}^{\text{gt}}) | x \in \mathcal{X}, \mathbf{Y}_{hw}^{\text{gt}} \in \mathcal{C}_S\}$, the iteration of seen class-guided learning T_g , the iteration of pseudo-guided learning T_p , self-training iterations T_s , up-sampling operator \mathcal{R}_u , downsampling operator \mathcal{R}_d ;

Phase 1: Seen class-guided learning

```

for  $t = 1, 2, \dots, T_g$  do
     $\mathbf{Y}^*, \mathbf{S}^* \leftarrow$  model prediction from  $Z_t(x)$ ;
     $\mathcal{L} \leftarrow \lambda_{\text{seg}} \mathcal{L}_{\text{seg}}(\mathbf{Y}^*, \mathbf{Y}^{\text{gt}})$ 
         $+ \lambda_{\text{score}} \mathcal{L}_{\text{score}}(\mathcal{M}(\mathbf{S}_L^*), \mathcal{R}_d(\mathbf{Y}^{\text{gt}}))$ ;
     $Z_{t+1} \leftarrow$  AdamW model parameter update;
    
```

Phase 2: Pseudo-guided learning;

```

for  $x, y$  in  $D$  do
    if  $\mathbf{Y}_{hw}^{\text{gt}} \notin \mathcal{C}_S$  then
         $\mathbf{Y}_{hw}^{\text{gt}} = \arg \max_{c \in \mathcal{C}_U} Z_{T_g}(\mathcal{R}_u(\mathcal{M}(\mathbf{S}^*)))_{hw} = c | x$ ;
    
```

for $t = T_g + 1, T_g + 2, \dots, T_p$ **do**

```

     $\mathbf{Y}^*, \mathbf{S}^* \leftarrow$  model prediction from  $Z_t(x)$ ;
     $\mathcal{L} \leftarrow \lambda_{\text{seg}} \mathcal{L}_{\text{seg}}(\mathbf{Y}^*, \mathbf{Y}^{\text{gt}})$ 
         $+ \lambda_{\text{score}} \mathcal{L}_{\text{score}}(\mathcal{M}(\mathbf{S}_L^*), \mathcal{R}_d(\mathbf{Y}^{\text{gt}}))$ ;
     $Z_{t+1} \leftarrow$  AdamW model parameter update;
    
```

Phase 3: Self-training

```

for  $t = T_p + 1, T_p + 2, \dots, T_p + T_s$  do
     $\mathbf{Y}^*, \mathbf{S}^* \leftarrow$  model prediction from  $Z_t(x)$ ;
    if  $\mathbf{Y}_{hw}^{\text{gt}} \notin \mathcal{C}_S$  then
         $\mathbf{Y}_{hw}^{\text{gt}} = \arg \max_{c \in \mathcal{C}_U} Z_{t-1}(\mathcal{R}_u(\mathcal{M}(\mathbf{S}^*)))_{hw} = c | x$ ;
     $\mathcal{L} \leftarrow \lambda_{\text{seg}} \mathcal{L}_{\text{seg}}(\mathbf{Y}^*, \mathbf{Y}^{\text{gt}})$ 
         $+ \lambda_{\text{score}} \mathcal{L}_{\text{score}}(\mathcal{M}(\mathbf{S}_L^*), \mathcal{R}_d(\mathbf{Y}^{\text{gt}}))$ ;
     $Z_{t+1} \leftarrow$  AdamW model parameter update;
    
```

Algorithm 2 Optimal Transport with Sinkhorn algorithm

Given: $\mu = \mathbf{1}^M / M, \nu = \mathbf{1}^N / N$, the score matrix \hat{S} ;

Input : The cost matrix $\mathbf{C} = \mathbf{1} - \hat{S}$, hyper-paramter λ , the max iteration t_{max} ;

Initialization: $\mathbf{K} = \exp(-\mathbf{C}/\lambda)$, $t \leftarrow 1, \mathbf{b}^0 = \mathbf{1}$;

1 **while** $t \leq t_{\text{max}}$ and not converge **do**

2 $\mathbf{a}^t = \mu / (\mathbf{K} \mathbf{b}^{t-1})$;

$\mathbf{b}^t = \nu / (\mathbf{K}^\top \mathbf{a}^t)$;

Output : Optimal transport plan $\mathbf{T}^* = \text{diag}(\mathbf{a})^t \mathbf{K} \text{diag}(\mathbf{b})^t$;

Table 5. Notation of the baseline and our proposed method

Model	DLFA	MPOT	Decoder Output	Intermediate Score maps	Final Score map
Our baseline	✓	✗	$\hat{\mathbf{Y}}$	$\{\hat{\mathbf{S}}_i\}_{i=1}^L$	$\hat{\mathbf{S}}_L$
ZegOT-Shallow	✓	Shallow	\mathbf{Y}^*	$\{\hat{\mathbf{S}}_i\}_{i=1}^L$	\mathbf{S}_L^* in (8)
ZegOT-Deep	✓	Deep	\mathbf{Y}^*	$\{\hat{\mathbf{S}}_i\}_{i=1}^L$	\mathbf{S}_L^* in (9)

loss, which are given by:

$$\mathcal{L}_{\text{CE}} = -\frac{1}{HW} \sum_{i=1}^{HW} \mathbf{Y}_i^{\text{gt}} \log(\phi(\mathbf{Y}_i^*)) + (1 - \mathbf{Y}_i^{\text{gt}}) \log(1 - \phi(\mathbf{Y}_i^*)), \quad (16)$$

$$\mathcal{L}_{\text{focal}} = -\frac{1}{HW} \sum_{i=1}^{HW} \mathbf{Y}_i^{\text{gt}} (1 - \sigma(\mathbf{Y}_i^*))^\gamma \log(\sigma(\mathbf{Y}_i^*)) + (1 - \mathbf{Y}_i^{\text{gt}}) \sigma(\mathbf{Y}_i^*)^\gamma \log(1 - \sigma(\mathbf{Y}_i^*)), \quad (17)$$

$$\mathcal{L}_{\text{dice}} = 1 - \frac{2 \sum_{i=1}^{HW} \mathbf{Y}_i^{\text{gt}} \mathbf{Y}_i^*}{\sum_{i=1}^{HW} \mathbf{Y}_i^{\text{gt}^2} + \sum_{i=1}^{HW} \mathbf{Y}_i^{*^2}}, \quad (18)$$

$$(19)$$

where \mathbf{Y}^* is the model decoder outputs of the decoder, \mathbf{Y}^{gt} is the ground truth label, $\phi(\cdot)$ and $\sigma(\cdot)$ are Softmax and Sigmoid operations, respectively; γ is a hyper-parameter to balance hard and easy samples, which is set to 2. Throughout the entire experiments, λ_{CE} , λ_{focal} , and λ_{dice} are set to 1, 20, and 1, respectively. In (14), both λ_{seg} and λ_{score} are set to 1. The above losses are for computing \mathcal{L}_{seg} in (12), and when to compute $\mathcal{L}_{\text{score}}$, the input \mathbf{Y}^* and the ground truth \mathbf{Y}^{gt} are replaced by $\mathcal{M}(\mathbf{S}_L^*)$ and $\mathcal{R}_d(\mathbf{Y}^{\text{gt}})$, respectively, where .

F. Details of Dataset

We utilize a total of three datasets, *i.e.*, PASCAL VOC 2012 (Everingham & Winn, 2012), PASCAL Context (Motaghi et al., 2014), and COCO-Stuff164K (Caesar et al., 2018). We divide seen and unseen classes for each dataset, following the settings of previous methods (Bucher et al., 2019; Xu et al., 2021; Ding et al., 2022; Zhou et al., 2022a;d). PASCAL VOC 2012 consists of 10,582 / 1,449 images with 20 categories, for training / validation. The dataset is divided into 15 seen and 5 unseen classes. PASCAL Context is an extensive dataset of PASCAL VOC 2010 that contains 4,996 / 5,104 images for training / test with 60 categories. The dataset is categorized into 50 seen and 10 unseen classes. COCO-Stuff 164K is a large-scale dataset that consists of 118,287 / 5,000 images for training / validation with 171 classes. The dataset is categorized into 156 seen and 15 unseen classes.

Table 6. Zero-shot semantic segmentation performance (pAcc).

Settings	Method	PASCAL VOC 2012	PASCAL Context	COCO-Stuff 164K	#Param
Inductive (Seen supervised)	CaGNet	80.7	59.2	56.6	101M
	ZegFormer	-	-	-	41M
	zsseg	-	-	60.3	61M
	ZegCLIP	94.6	76.2	62.0	130M
Transductive w/ Self Training (Seen supervised + Unseen self-supervised)	CaGNet	81.6	59.6	56.8	101M
	STRICT	-	-	-	101M
	zsseg	-	-	-	61M
	MaskCLIP+	94.0	74.8	67.6	140M
	ZegCLIP	95.1	77.2	68.8	130M
	ZegOT-Shallow	95.6	80.9	65.7	21M
	ZegOT-Deep	96.0	80.8	64.2	21M

Table 7. Component analysis of hyper-parameter of our method. # denotes the hyper-parameters of configurations. Checkmark ✓ indicates that the default configuration of ZegOT.

Components	#	mIoU (S)	mIoU (U)	hIoU	ZegOT
Context length (l)	8	91.9	91.6	91.7	✓
	16	92.2	89.6	90.9	
	32	91.9	90.3	91.1	
Score matrix weight (w)	0.6	91.0	91.4	91.2	
	0.7	91.0	91.5	91.3	
	0.8	91.9	91.6	91.7	✓
	0.9	91.5	91.7	91.6	
	1.0	89.5	88.4	88.9	

G. Implementation Detail

We further declare the implementation detail for our work. Input image resolution is set as 480×480 for PASCAL Context, and 512×512 for the rest of the datasets. The context length is set to 8 and the weight w for the score matrix (15) is set to 0.8. We choose the lightest training schedule, which is 20K / 40K / 80K for PASCAL VOC 2012 / PASCAL Context / COCO-Stuff-164K.

H. Definition of Harmonic mean IoU

Following the previous works (Xu et al., 2021; Zhou et al., 2022a;d), we define harmonic mean IoU (hIoU) among the seen and unseen classes as:

$$\text{hIoU} = \frac{2 * \text{mIoU}(\text{S}) + \text{mIoU}(\text{U})}{\text{mIoU}(\text{S}) + \text{mIoU}(\text{U})} \quad (20)$$

I. Quantitative Analysis on Zero-Shot Segmentation Performance

We further report pixel-wise classification accuracy (pAcc) compared to baseline methods similar with Table 2.

J. Further Analysis on Hyper-parameters.

Similar to Table 4, we further conduct the component analysis with varying hyper-parameters including: context length (l), and score matrix weight (w). Firstly, we empirically find that the large context length is limited to take significant effect on segmentation performance, *e.g.*, when $l = 16$, the performance on seen classes is the best, but the performance on unseen classes drops. Since we consider the hIoU as a major metric, we adopt $l = 8$ as the default setting.

We further investigate the effect of the score matrix weight, which is described in Eq. (15) for the network inference. We observe that ZegOT performs the best when $w = 0.8$, but the performance gradually drops when w is further decreased or increased. In addition, we find that the segmentation performance on both seen and unseen classes significantly drops when $w = 1.0$, which means that \mathbf{Y}^* is also important to predict the final segmentation maps.

K. Additional Visual Results.

We provide additional visual results. Fig. 7 and Fig. 8 show qualitative zero-shot segmentation performance of our ZegOT and the baseline method for COCO-Stuff164K, PASCAL VOC 2012 and PASCAL Context datasets. Fig. 9 shows additional visual results of text prompt-related score matrix on PASCAL VOC 2012 dataset.

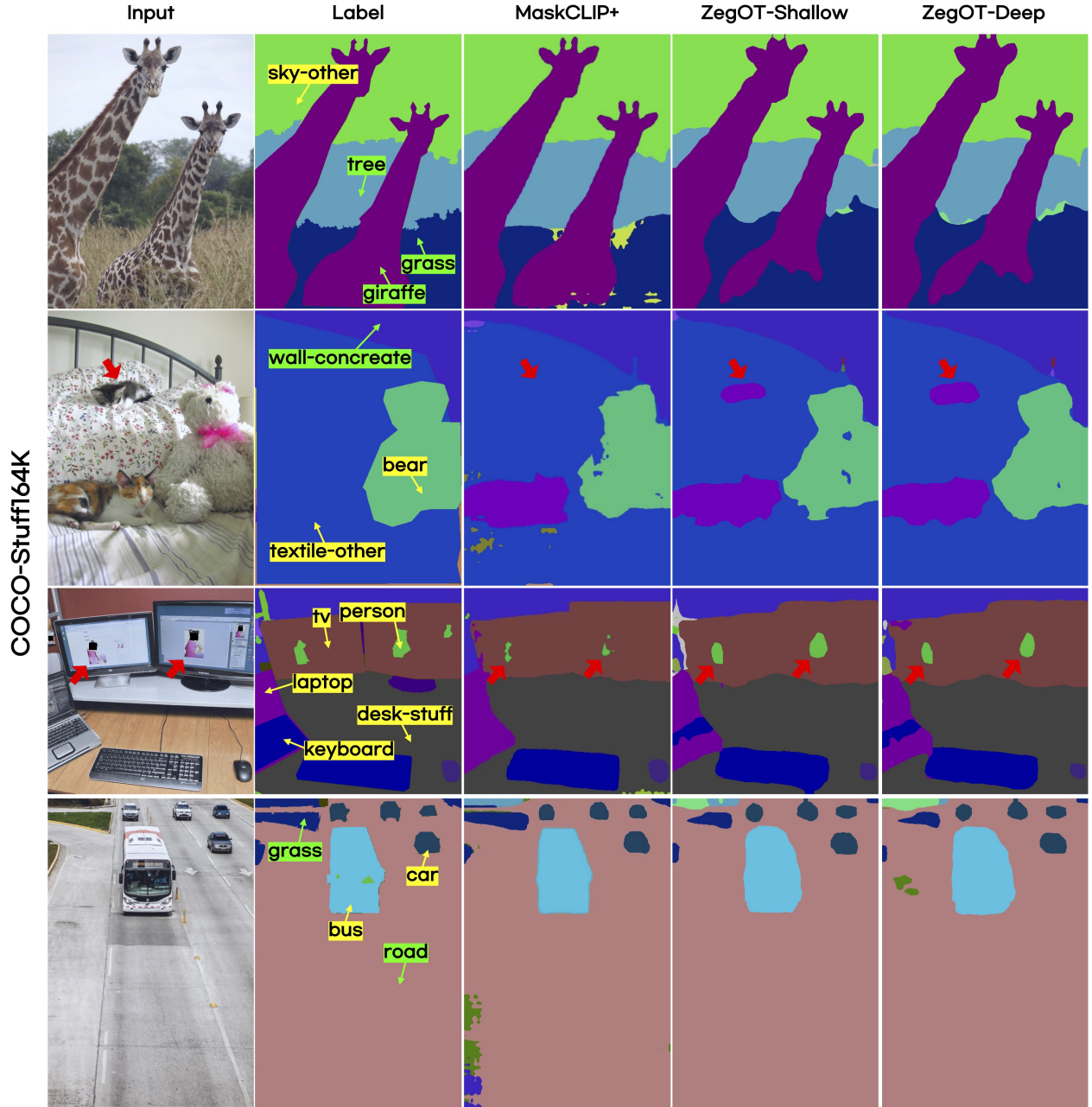


Figure 7. Qualitative zero-shot segmentation results on COCO-Stuff164K dataset. The yellow tag indicates seen classes, while the green tag indicates unseen classes. Surprisingly, our ZegOT-Shallow and ZegOT-Deep effectively segment a tiny cat that does not even belong to the ground truth (see red arrows in 2nd row), and properly segment the person class within the small-sized portraits (see red arrows in 3rd row), while the previous SOTA method shows inferior performance on these features.

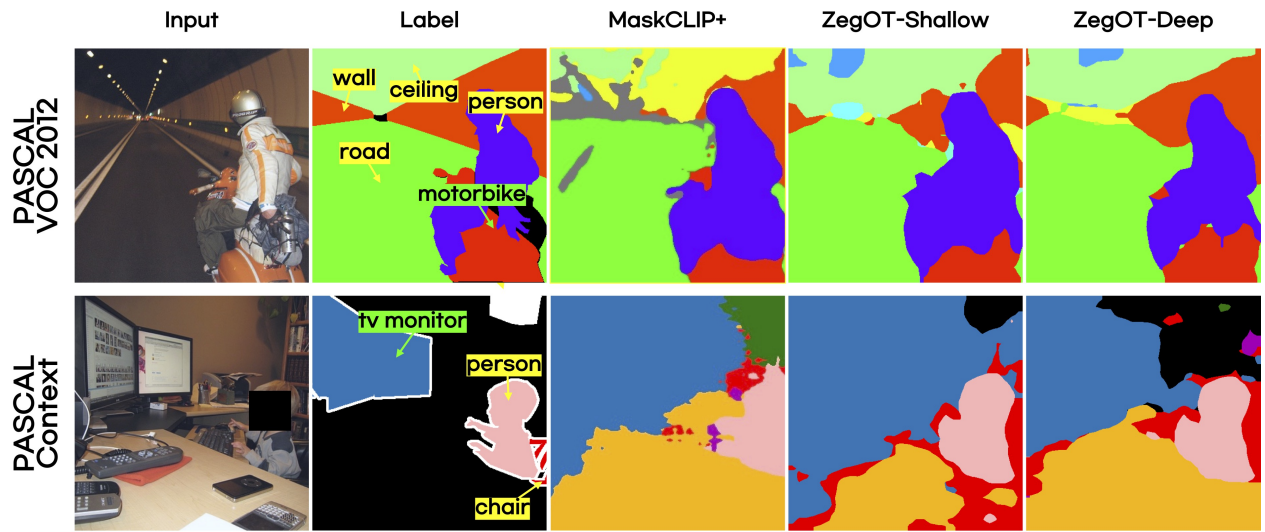


Figure 8. Qualitative zero-shot segmentation results on PASCAL VOC 2012 and PASCAL Context datasets. The yellow tag indicates seen classes, while the green tag indicates unseen classes.

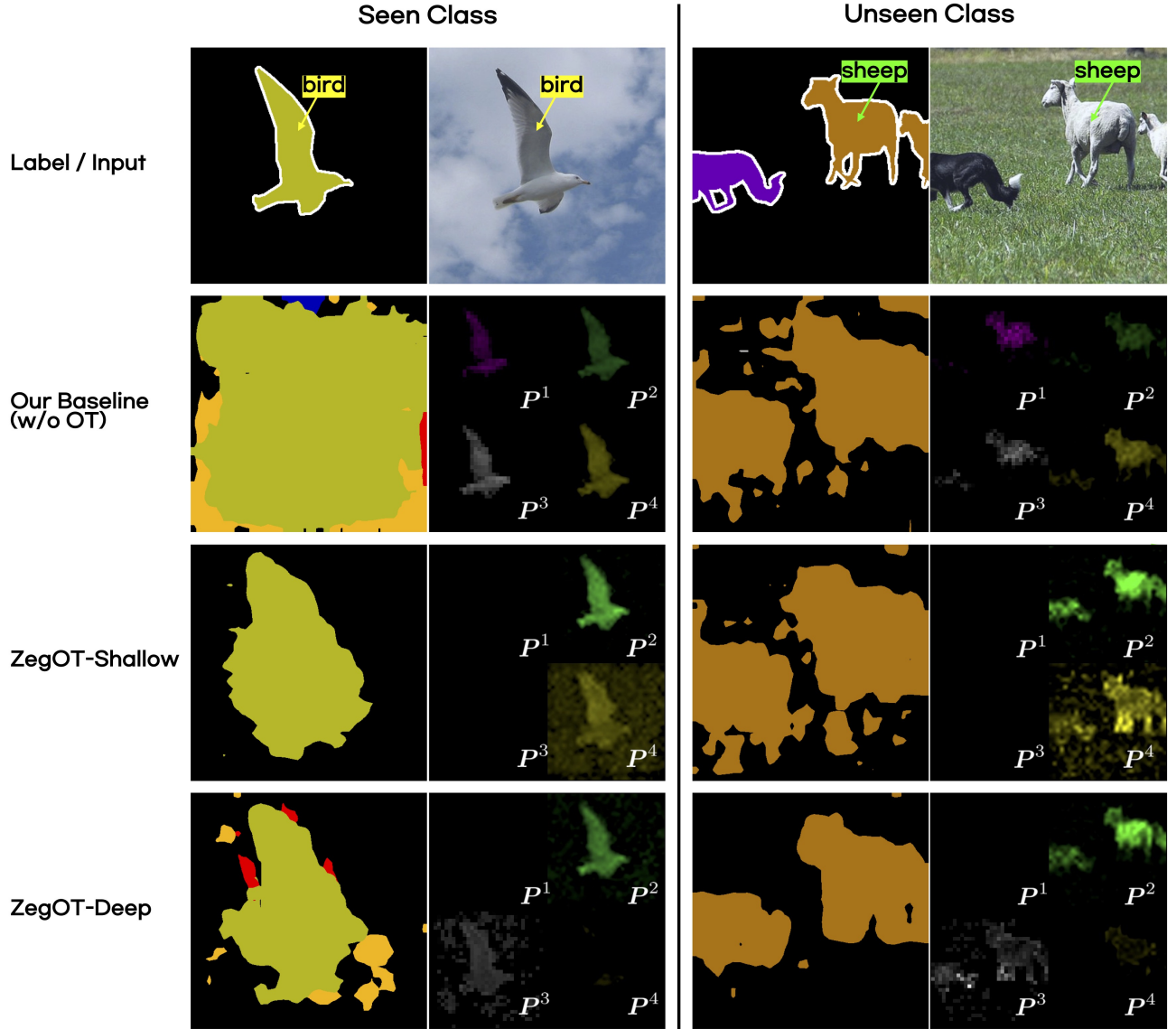


Figure 9. Visualization of the learned text prompt and image pixel alignment. The yellow tag indicates seen classes, while the green tag indicates unseen classes. For each method, we present its segmentation result (left) and N multiple text prompts-related score matrix activated by the predicted class (right). In the baseline method without OT, all the P^i -related score matrices resemble each others. On the other hand, our ZegOT-Shallow and ZegOT-Deep show separate score matrices, with ZegOT-Deep more focusing on different semantic attributes of the predicted class object.